Climate Modelling User Group

Deliverable 3.1c - Scientific Report for WP5.3

Impact of integrating CCI LC data in the ISBA land surface model

Centres providing input: Météo-France

Revision nr.	Date	Status
1.0	27 May 2025	First version by JC Calvet and O Rojas-Munoz
2.0	13 June 2025	Revised version

CMUG CCI+ Deliverable 5.3.3

Interim Progress Report

Table of Contents

Impact of integrating CCI LC data in the ISBA land surface model

1. Purpose and scope of this report

This document is a scientific report on a Cross-ECV climate science study dedicated to the assessment of the impact of integrating CCI land cover (LC) data in the Interactions between Soil, Biosphere, Atmosphere (ISBA) land surface model of Météo-France. Its purpose is to assess the impact on simulated soil moisture (SM), land surface temperature (LST), and snow water equivalent (SWE) of updating land cover (LC) information in ISBA using CCI LC products in the SURFEX (Surface externalisée) modelling platform of Météo-France (Masson et al. 2013, Le Moigne and Minvielle 2020) that includes the ISBA model. CCI SWE, SM, and LST products are used as a benchmark. In SURFEX, spatially variable model parameters are generated using the ECOCLIMAP tool (Masson et al. 2003). This tool is used to convert land cover classes into functional vegetation types and to calculate the fraction covered by these types according to the spatial resolution used by the model. In addition to this information on vegetation, digital maps describing relief and soil properties such as sand and clay fractions are available in SURFEX. LC information in land surface models is often based on quite old EO observations and classifications. Quantifying the added value of regularly updated LC is a key question. CNRM has recently developed a new version of the land cover algorithm in SURFEX, called ECOCLIMAP-SG. Compared to the old ECOCLIMAP, ECOCLIMAP-SG is able to ingest CCI land cover maps at a spatial resolution of 300m. Comparing simulations using the new and the old ECOCLIMAP versions allows the assessment of the impact of CCI LC on the simulations of the CCI SM, LST and SWE products. This evaluation contributes to examine the following questions: (1) How do LC uncertainties propagate to the water and energy budgets? (2) Can Earth observation (EO) data improve land reanalyses?

2. Approach for assessing the impact of CCI LC data in ISBA

The work is focused over Eurasia at a spatial resolution of 0.25 x 0.25° from 2010 to 2022. The experimental and validation protocol is presented in Table 1, which includes the CCI product being assessed (LC), and those used as a benchmark (LST, SM, SWE). Table 1 lists the five numerical experiments that were conducted. In this study, the ISBA model uses the ERA5 atmospheric forcing. The ISBA configuration used includes interactive Leaf Area Index (LAI) simulation.

Table 1: Main features of CMUG WP5.3 on assessing the impact of integrating CCI LC land cover data in the ISBA land surface model on several Essential Climate Variables (ECVs).

CMUG WP 5.3: Assessment of the impact of CCI LC, Eurasia, 2010-2022		Experiment type	CCI ECVs	Version of CCI ECVs
1	ISBA using pre-existing LC	Reanalysis	-	-
2	ISBA using CCI LC	Reanalysis	LC	LC v2.0.7 1992-2015
3	Comparison of simulated LST	Benchmarking	LST	V4 AQUA_MODIS_L3C_0.05, TERRA_MODIS_L3C_0.05
4	Comparison of simulated SM	Benchmarking	SM	SM COMBINED v8.1
5	Comparison of simulated SWE	Benchmarking	SWE	V2.0, V3.0, V3.1

3. CMUG WP5.3 Results

3.1 CCI LC vs. pre-existing geographical information in SURFEX

Figure 1 presents two maps of the dominant land cover type over Eurasia at a spatial resolution of 0.25° x 0.25°, derived from ECOCLIMAP-II (Faroux et al. 2013), and from ECOCLIMAP-SG (Calvet and Champeaux 2020) with versions v2.0.7 of CCI LC.
Major differences are observed between ECOCLIMAP-II and ECOCLIMAP-SG, with less bare soil, more forests, and more crops in ECOCLIMAP-SG.

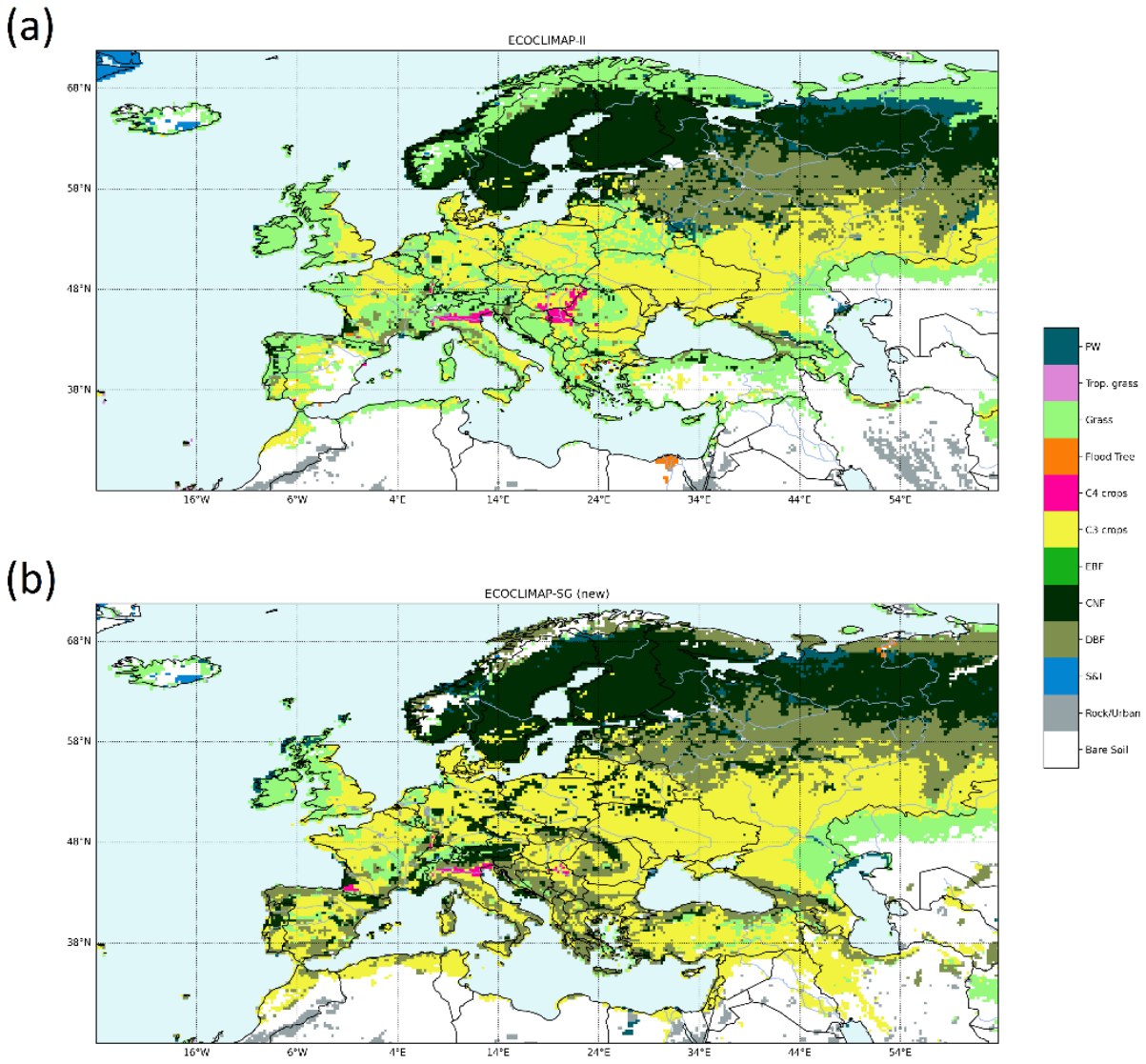

***Figure 1**: Dominant land cover type over Eurasia at a spatial resolution of 0.25° x 0.25° as derived from (a) ECOCLIMAP-II (Faroux et al. 2013), (b) ECOCLIMAP-SG (Calvet and Champeaux 2020) with LC v2.0.7 1992-2015. The 12 dominant land cover types are indicated in the colour bar from top to bottom: peat and wetlands, tropical grasslands, temperate grasslands, flooded trees/irrigation, C4 crops (e.g. maize), C3 crops (e.g. wheat), broadleaf evergreen trees, coniferous trees, deciduous broadleaf trees, permanent snow and ice, rocks/urban.*

3.2 ISBA simulations

ISBA simulation results are presented in Fig. 2 for pre-existing LC (feature 1 in Table 1), i.e. using ECOCLIMAP-II.

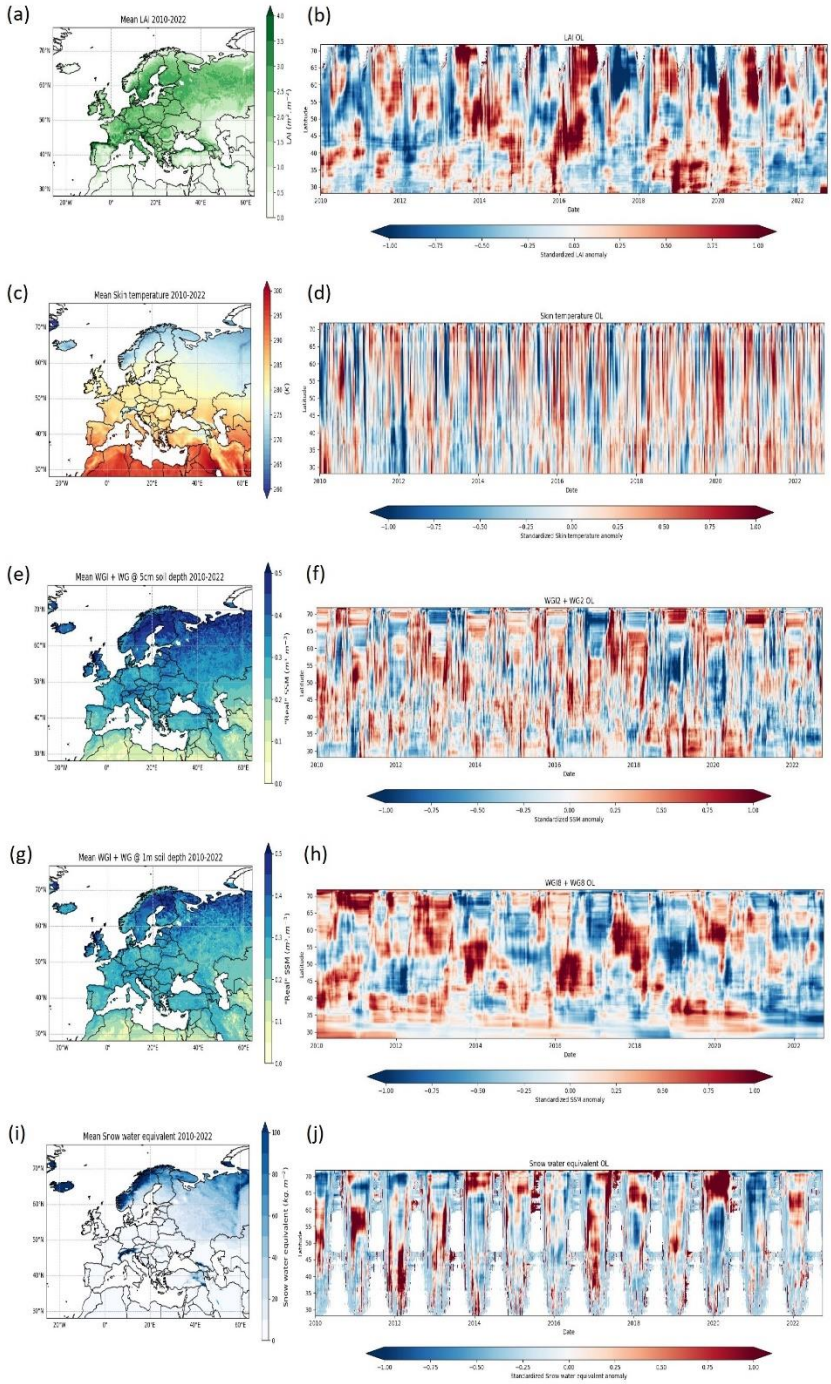

Figure 2*: ISBA simulations over Eurasia forced by ERA5 atmospheric variables from 2010 to 2022 at a spatial resolution of 0.25° x 0.25°. Mean values (a,c,e,g,i) and Hovmoller plot (b,d,f,h,j) of scaled anomalies of (a,b) LAI, (c,d) LST, (e,f) surface soil moisture, (g,h) deep soil moisture (0.8-1.0m), (i,j) SWE.*

3.3 Impact of new land cover on Leaf Area Index (LAI)

LAI is a major variable characterizing the vegetation canopy structure controlling evapotranspiration and the surface energy, water and carbon budgets. At high latitude, LAI seasonal and interannual variability can be related to a large extent to snow. Updating ECOCLIMAP with CCI LC has a major impact on the simulated LAI, as shown by Figure 3. Mediterranean regions have higher LAI values when using LC CCI, which is related to less bare soil. Urban areas have smaller LAI values in relation to larger cities and larger fractions of built-up areas.

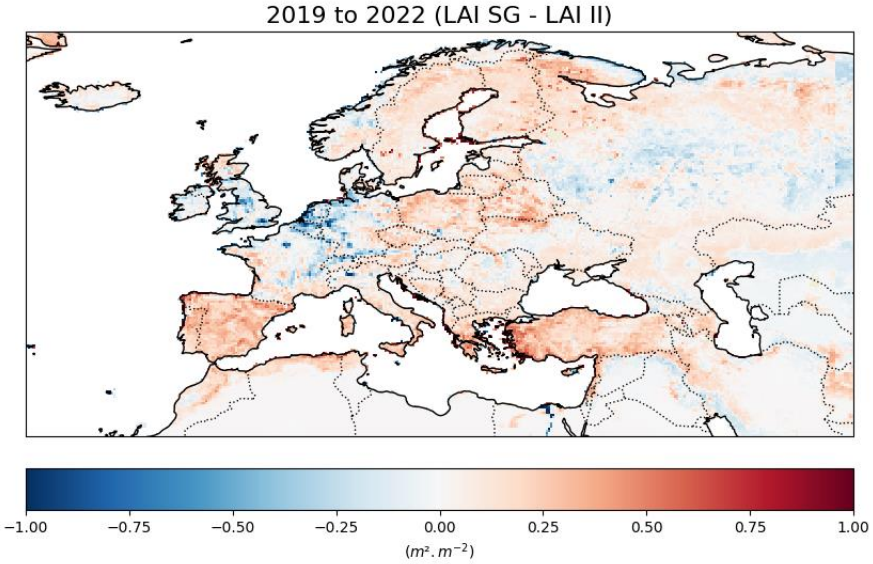

***Figure 3**: Mean LAI differences between ISBA simulations using CCI LC vs. pre-existing LC ("LAI SG" and "LAI II", respectively), from 2019 to 2022.*

3.4 Snow CCI SWE product vs. ISBA simulations

Figure 4 presents a comparison of time series of mean SWE values over Eurasia between CCI Snow and ISBA simulations with and without CCI LC. There is a good agreement between the observations and the ISBA simulations. However, the model presents larger peak SWE values and the difference between the annual peak SWE values exceeds 25 mm in 2014 and 2020. Figure 2 shows that 2014 and 2020 correspond to warm winters with positive anomalies of LAI and LST, positive anomalies of SWE at high latitudes (65-70°N) and negative anomalies of SWE at mid-latitudes (45-60°N). The rather large bias observed in these conditions needs to be investigated.

Figure 5 presents the geographical distribution of mean SWE values and CCI minus model differences. In spite of simulated SWE annual peaks larger than observed, the simulated mean SWE values are smaller than the CCI SWE in some regions such as Western Europe, Sweden, Finland.

The consistency of simulated SWE is assessed using CCI SWE observations in Table 2 for both ISBA simulations with and without CCI LC. Table 2 shows that using CCI LC slightly improves the Pearson correlation coefficient, rising from 0.70 to 0.71. The use of CCI LC has no impact on unbiased RMSD (ubRMSD) but markedly improves RMSD. The latter drops from 29.2 mm to 23.3 mm (Table 2).

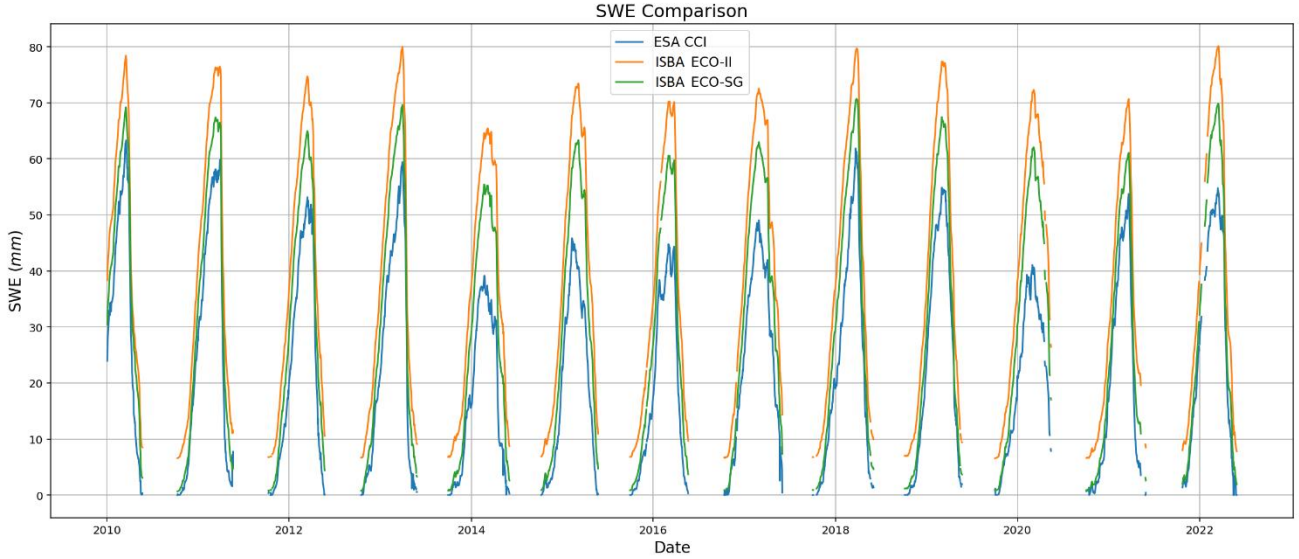

***Figure 4**: Mean SWE value over Eurasia from CCI Snow, ISBA simulations using CCI LC ("ECO-SG") and pre-existing LC ("ECO-II") from 2010 to 2022.*

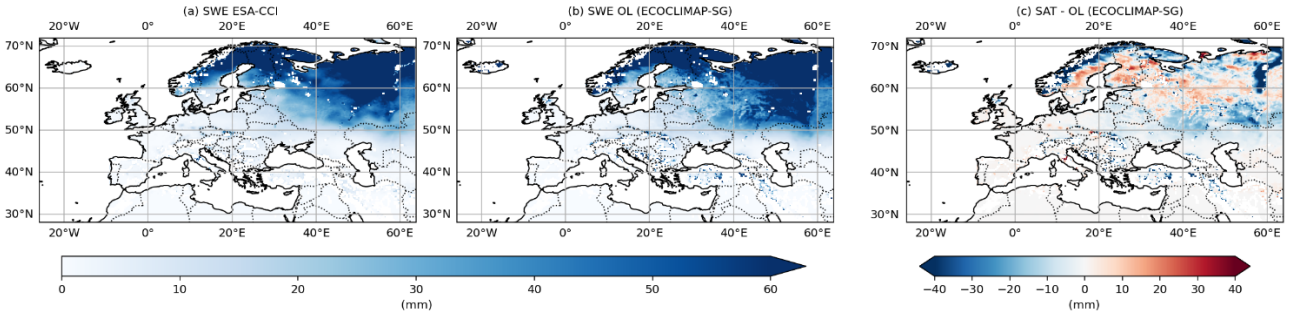

***Figure 5**: Map of mean SWE value over Eurasia from (a) CCI Snow, (b) ISBA simulations using CCI LC ("ECOCLIMAP-SG"), and (c) the difference between CCI Snow and ISBA simulations using CCI LC.*

Table 2: Mean of grid-cell level score values of ISBA SWE simulations using CCI LC and pre-existing LC from 2010 to 2022 with respect to CCI SWE observations.

CMUG WP 5.3: Assessment of the impact of CCI LC, Eurasia, 2010-2022		Mean Pearson correlation coefficient	Mean RMSD (mm)	Mean ubRMSD (mm)
1	ISBA using pre-existing LC	0.70	29.2	16.9
2	ISBA using CCI LC (ECOCLIMAP-SG)	0.71	23.3	16.9

Since the mean of grid-cell level score values shown in Table 2 may hide more complex spatial differences in the usefulness of CCI LC to improve SWE simulations, Fig. 6 shows maps of Pearson correlation coefficient and RMSD differences. While the use of CCI LC tends to improve these scores overall, both score values are degraded in some areas such as large parts of Sweden and Finland.

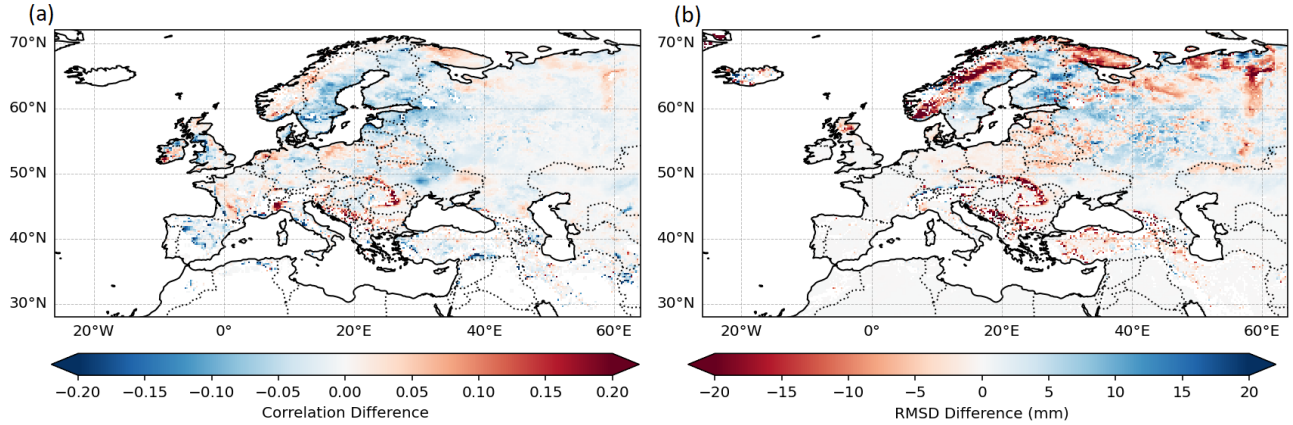

***Figure 6**: Score value differences of SWE ISBA simulations (CCI LC minus pre-existing LC) with respect to CCI SWE observations from 2010 to 2022: (a) Pearson correlation coefficient difference, (b) RMSD difference. Red colour corresponds to improved score values.*

Since ISBA SWE simulations tend to overestimate SWE (Fig. 4), it is important to check that simulated SWE anomalies are consistent with the observations. Figure 7 shows scaled anomalies (z-score) of simulated and observed SWE for the warm winter of 2020, for which a large model bias is observed. Most of the domain presents a negative SWE anomaly in 2020, consistent with the small mean SWE peak in Fig. 4. On the other hand, a positive SWE anomaly is observed for the northeastern part of the domain. The simulated SWE anomaly is consistent with the observed anomaly.

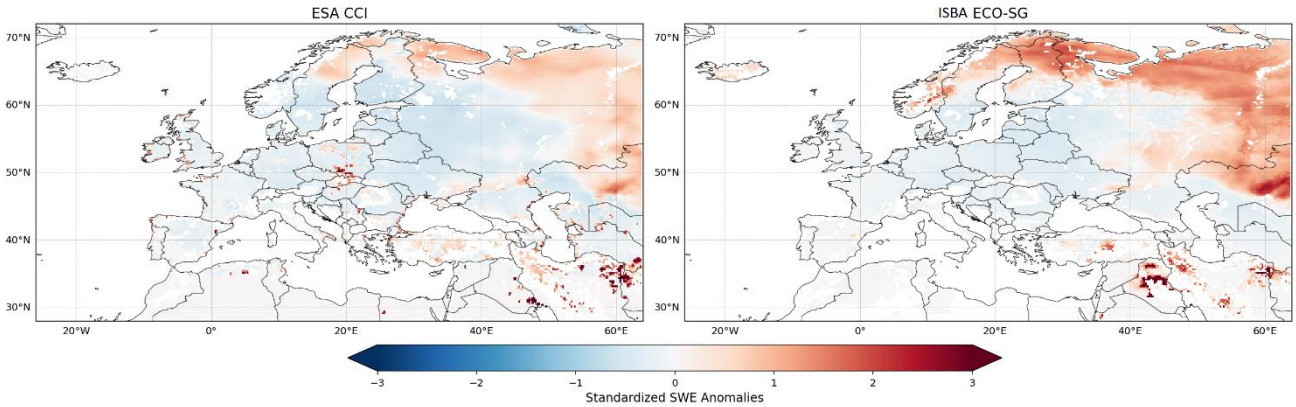

***Figure 7**: Scaled SWE anomaly for the warm winter of 2020 of: (left) CCI SWE observations, and (right) SWE ISBA simulations using CCI LC, from 2010 to 2022. Red colour corresponds to positive SWE anomalies.*

3.5 CCI SM product vs. ISBA simulations

Figure 8 presents a comparison of time series of mean normalized SM (surface soil moisture) values over Eurasia between CCI SM and ISBA simulations with and without CCI LC. There is a good agreement between the observations and the ISBA simulations. Figure 9 presents the geographical distribution of mean SM values and CCI minus model differences. In spite of simulated SM annual peaks being smaller than observed, the simulated mean SM values are larger than the CCI SM in some regions such as Sweden.

The consistency of simulated SM is assessed using CCI SM observations in Table 3 for both ISBA simulations with and without CCI LC. Table 3 shows that using CCI LC slightly degrades the Pearson correlation coefficient, dropping from 0.63 to 0.62. The use of CCI LC has no impact on other score values.

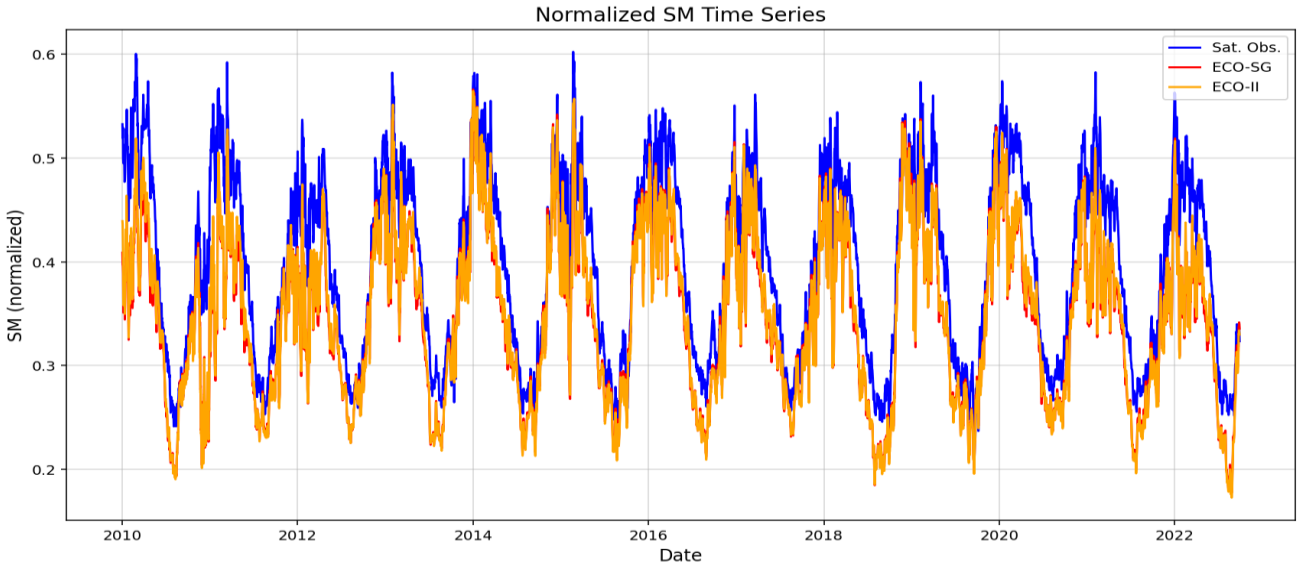

***Figure 8**: Mean normalized SM value over Eurasia from CCI SM, ISBA simulations using CCI LC ("ECO-SG") and pre-existing LC ("ECO-II") from 2010 to 2022.*

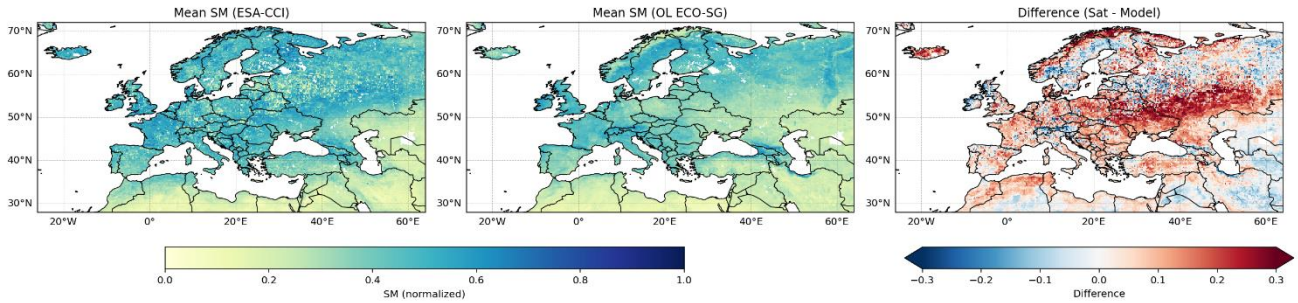

***Figure 9**: Map of mean normalized SM value over Eurasia from (left) CCI SM, (middle) ISBA simulations using CCI LC ("ECO-SG"), and (right) the difference between CCI SM and ISBA simulations using CCI LC.*

Table 3: Mean of grid-cell level score values of ISBA SM simulations using CCI LC and pre-existing LC from 2010 to 2022 with respect to CCI SM observations (normalized values).

CMUG WP 5.3: Assessment of the impact of CCI LC, Eurasia, 2010-2022		Mean Pearson correlation coefficient	Mean RMSD (-)	Mean ubRMSD (-)
1	ISBA using pre-existing LC	0.63	0.10	0.08
2	ISBA using CCI LC (ECOCLIMAP-SG)	0.62	0.10	0.08

3.6 CCI LST product vs. ISBA simulations

Figure 10 shows a comparison of the daytime and night-time time series of mean land surface temperature (LST) values over Western Europe and North Africa, comparing the CCI LST and ISBA simulations with and without CCI LC. The ISBA simulations show a significant cold bias during the day. Figure 11 shows the geographical distribution of mean LST values and the difference between CCI and the model. The daytime cold bias is observed across all of Western Europe, particularly in Spain and North Africa. At night, a moderate warm bias is generally observed, with larger values at high latitudes. The consistency of the simulated LST is assessed using the CCI LST observations for daytime and night-time in Tables 4 and 5, respectively, for both the ISBA simulations with and without CCI LC. Using CCI LC improves the consistency of the model with the CCI LST observations at nighttime. During the day, mean RMSD and ubRMSD tend to worsen slightly.

Table 4: Mean of grid-cell level score values of daytime ISBA LST simulations using CCI LC and pre-existing LC from 2010 to 2022 with respect to CCI LST observations.

CMUG WP 5.3: Assessment of the impact of CCI LC, Eurasia, 2010-2022		Mean Pearson correlation coefficient	Mean RMSD (K)	Mean ubRMSD (K)
1	ISBA using pre-existing LC	0.86	6.5	4.4
2	ISBA using CCI LC (ECOCLIMAP-SG)	0.86	6.7	4.5

Table 5: Mean of grid-cell level score values of nighttime ISBA LST simulations using CCI LC and pre-existing LC from 2010 to 2022 with respect to CCI LST observations.

CMUG WP 5.3: Assessment of the impact of CCI LC, Eurasia, 2010-2022		Mean Pearson correlation coefficient	Mean RMSD (K)	Mean ubRMSD (K)
1	ISBA using pre-existing LC	0.90	3.5	2.5
2	ISBA using CCI LC (ECOCLIMAP-SG)	0.90	3.0	2.4

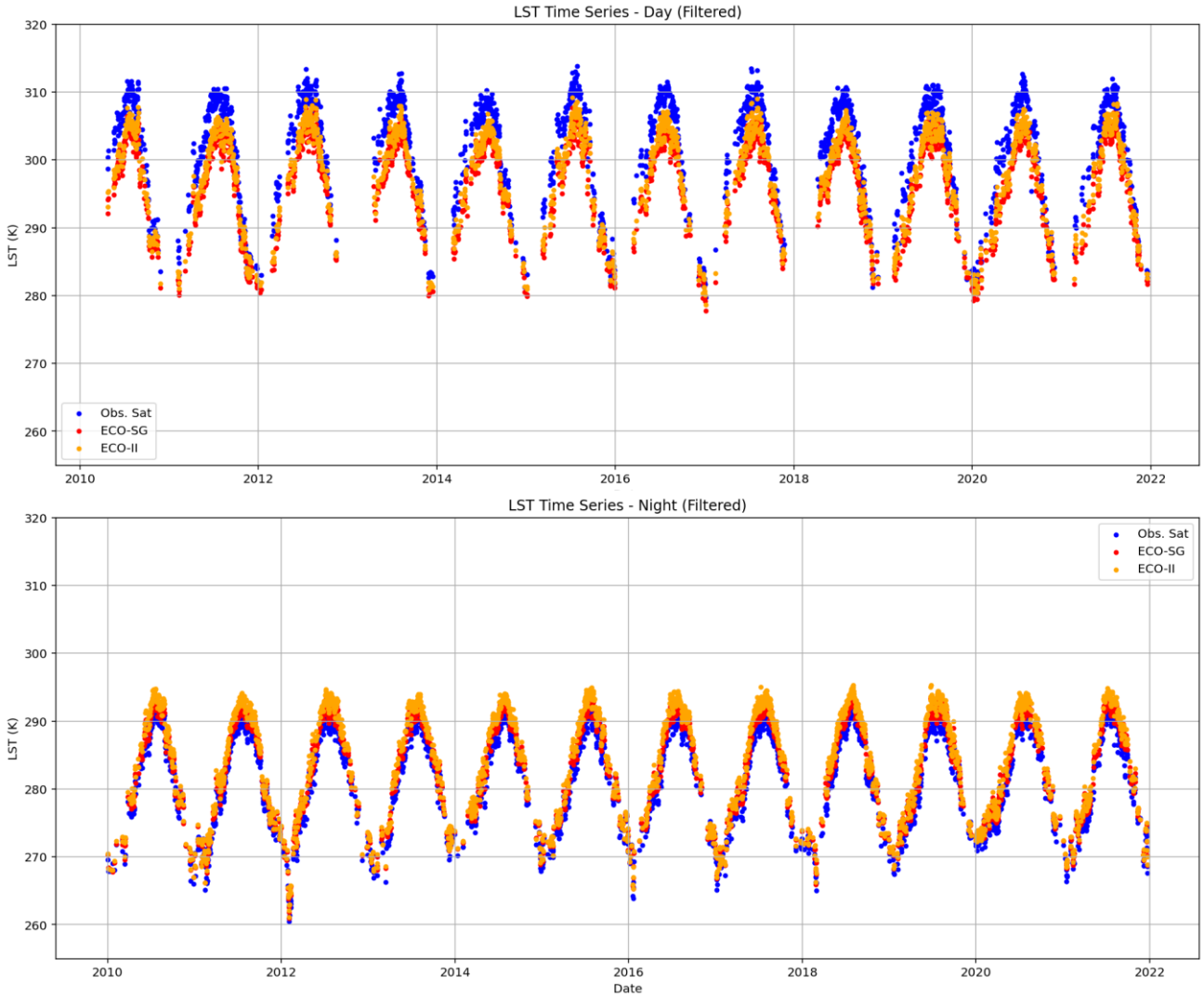

***Figure 10**: Mean LST value over Western Europe from CCI LST, ISBA simulations using CCI LC ("ECO-SG") and pre-existing LC ("ECO-II") from 2010 to 2022: (top) daytime values at 10h00 local time, (bottom) nighttime at 22h00 local time, corresponding to ISBA simulations at 09h00 and 21h00 UTC, respectively.*

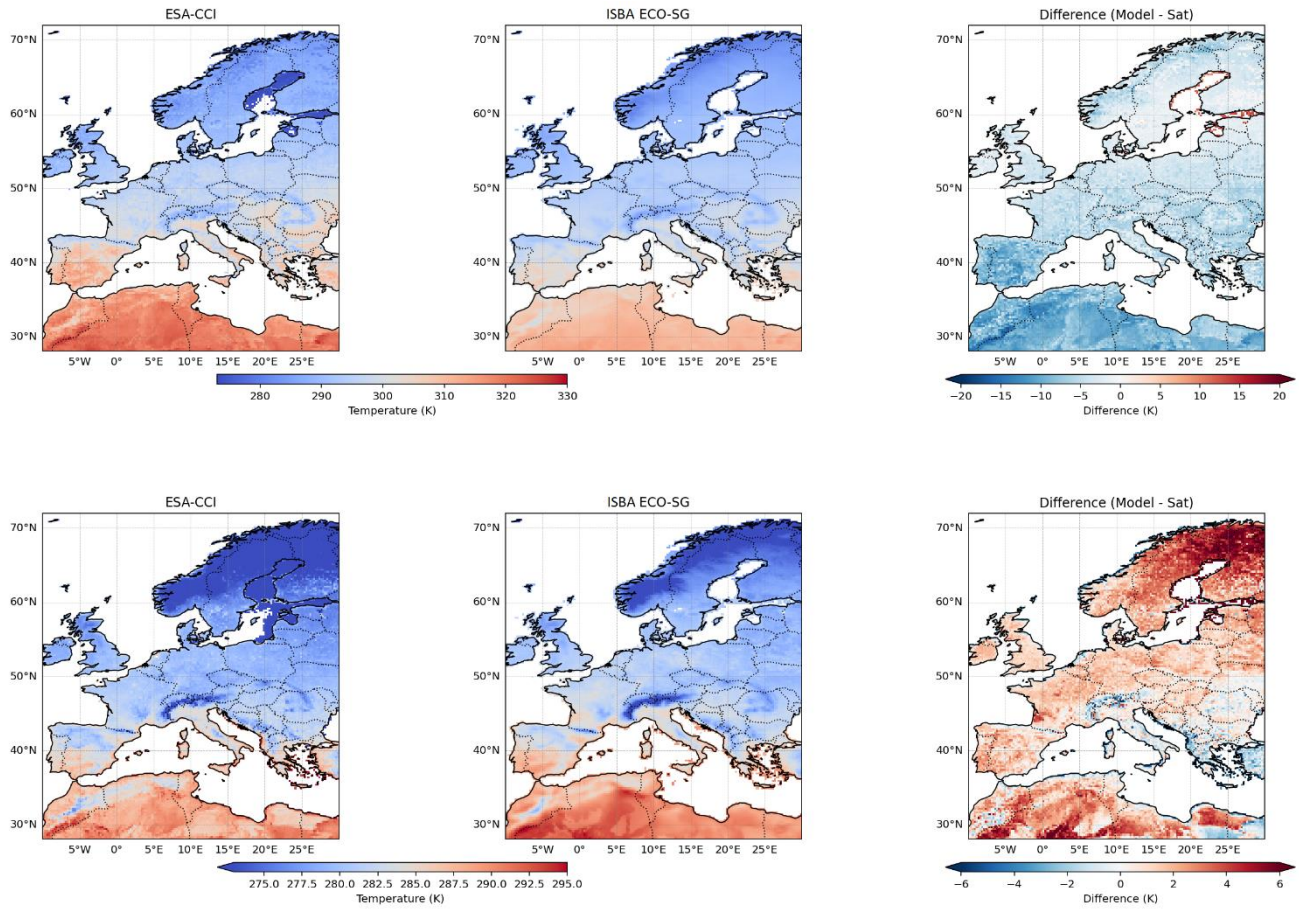

***Figure 11**: Maps of mean (top) daytime and (bottom) nighttime LST value over Western Europe and North Africa from (left) CCI LST, (middle) ISBA simulations using CCI LC ("ECO-SG"), and (right) the difference between CCI LST and ISBA simulations using CCI LC.*

4. Conclusions

The ISBA land surface model simulated land surface variables over Eurasia at a spatial resolution of 0.25° x 0.25° from 2010 to 2022. Simulations were performed with and without CCI LC. The simulated snow water equivalent (SWE), soil moisture (SM) and land surface temperature (LST) were compared with the CCI SWE, SM and LST observations. Using CCI LC in ISBA improved the model's consistency with CCI observations for SWE and night-time LST, demonstrating that LC uncertainties can affect the water and energy budgets. This study also shows that ISBA, when forced by ERA5, exhibits a significant daytime LST cold bias of 4.5 K, and that SWE is generally overestimated. This key result shows that CCI data can help identify model shortcomings. However, the use of CCI LC may degrade ISBA simulations of SWE in some areas of Scandinavia.

5. References

Albergel, C., Zheng, Y., Bonan, B., Dutra, E., Rodríguez-Fernández, N., Munier, S., Draper, C., de Rosnay, P., Muñoz-Sabater, J., Balsamo, G., Fairbairn, D., Meurey, C., and Calvet, J.-C.: Data assimilation for continuous global assessment of severe conditions over terrestrial surfaces, Hydrol. Earth Syst. Sci., 24, 4291–4316, https://doi.org/10.5194/hess-24-4291-2020, 2020.

Calvet, J.-C. and Champeaux J.-L.: L'apport de la télédétection spatiale à la modélisation des surfaces continentales, La Météorologie, 108, 52–58, https://doi.org/10.37053/lameteorologie-2020-0016, 2020.

Faroux, S., Kaptué Tchuenté, A. T., Roujean, J.-L., Masson, V., Martin, E., and Le Moigne, P.: ECOCLIMAP-II/Europe: a twofold database of ecosystems and surface parameters at 1 km resolution based on satellite information for use in land surface, meteorological and climate models, Geosci. Model Dev., 6, 563–582, https://doi.org/10.5194/gmd-6-563-2013, 2013.

Le Moigne P., Minvielle M.: SURFEX : une plateforme pour simuler les flux des surfaces océaniques et continentales, La Météorologie, 108, 82-87, https://doi.org/10.37053/lameteorologie-2020-0020, 2020.

Masson V., Champeaux J.-L., Chauvin F., Meriguet C., Lacaze R.: A global database of land surface parameters at 1-km resolution in meteorological and climate models. J. Climate, 16, 1261-1282, https://doi.org/10.1175/1520-0442-16.9.1261, 2003.

Masson V., Le Moigne P., Martin E., Faroux S., Alias A., Alkama R., Belamari S., Barbu A., Boone A., Bouyssel F., Brousseau P., Brun E., Calvet J.-C., Carrer D., Decharme B., Delire C., Donier S., Essaouini K., Gibelin A.-L., Giordani H., Habets F., Jidane M., Kerdraon G., Kourzeneva E., Lafaysse M., Lafont S., Lebeaupin-Brossier C., Lemonsu A., Mahfouf J.-F., Marguinaud P., Mokhtari M., Morin S., Pigeon G., Salgado R., Seity Y., Taillefer F., Tanguy G., Tulet P., Vincendon B., Vionnet V., Voldoire A.: The SURFEXv7.2 land and ocean surface platform for coupled or offline simulation of earth surface variables and fluxes. Geosci. Model Dev., 6, 929-960, https://doi.org/10.5194/gmd-6-929-2013, 2013.